

## In-Medium Effects on Phase Space Distributions of Antikaons Measured in Proton-Nucleus Collisions

W. Scheinast,<sup>6</sup> I. Böttcher,<sup>4</sup> M. Dębowski,<sup>5,6</sup> F. Dohrmann,<sup>6</sup> A. Förster,<sup>2,\*</sup> E. Grosse,<sup>6,7</sup> P. Koczoń,<sup>1</sup> B. Kohlmeier,<sup>4</sup> F. Laue,<sup>1,†</sup> M. Menzel,<sup>4</sup> L. Naumann,<sup>6</sup> E. Schwab,<sup>1</sup> P. Senger,<sup>1</sup> Y. Shin,<sup>3</sup> H. Ströbele,<sup>3</sup> C. Sturm,<sup>2,1</sup> G. Surówka,<sup>1,5</sup> F. Uhlig,<sup>2,1</sup> A. Wagner,<sup>6</sup> W. Waluś,<sup>5</sup> B. Kämpfer,<sup>6</sup> and H. W. Barz<sup>6</sup>

(KaoS Collaboration)

<sup>1</sup>*Gesellschaft für Schwerionenforschung, D-64220 Darmstadt, Germany*

<sup>2</sup>*Technische Universität Darmstadt, D-64289 Darmstadt, Germany*

<sup>3</sup>*Johann Wolfgang Goethe-Universität, D-60325 Frankfurt am Main, Germany*

<sup>4</sup>*Phillips Universität, D-35037 Marburg, Germany*

<sup>5</sup>*Jagiellonian University, PL-30059 Kraków, Poland*

<sup>6</sup>*Forschungszentrum Rossendorf, D-01314 Dresden, Germany*

<sup>7</sup>*Technische Universität Dresden, D-01062 Dresden, Germany*

(Received 3 February 2005; published 24 February 2006)

Differential production cross sections of  $K^\pm$  mesons have been measured in  $p + C$  and  $p + Au$  collisions at 1.6, 2.5, and 3.5 GeV proton beam energy. At beam energies close to the production threshold, the  $K^-$  multiplicity is strongly enhanced with respect to proton-proton collisions. According to microscopic transport calculations, this enhancement is caused by two effects: the strangeness exchange reaction  $NY \rightarrow K^- NN$  and an attractive in-medium  $K^- N$  potential at saturation density.

DOI: [10.1103/PhysRevLett.96.072301](https://doi.org/10.1103/PhysRevLett.96.072301)

PACS numbers: 25.75.Dw, 25.40.Ve

The past decade witnessed substantial experimental and theoretical efforts in the study of in-medium properties of strange particles. A large body of new data on the production of kaons and antikaons in nucleus-nucleus collisions at beam energies below or close to the nucleon-nucleon ( $NN$ ) threshold has been collected. It was found that the  $K^-/K^+$  ratio is enhanced in heavy-ion collisions as compared to proton-proton collisions [1–4]. The enhanced production of  $K^-$  mesons per number of participants was found to be partly due to strangeness exchange reactions ( $\pi Y \rightarrow K^- N$ , with  $Y = \Lambda, \Sigma$ ) which are strongly suppressed in  $p + p$  reactions. The measured kaon and antikaon yields can only be reproduced by transport model calculations when taking into account density-dependent  $K$  meson nucleon ( $KN$ ) potentials parametrizing effectively the in-medium modification of the  $K$  mesons [5,6]. The pronounced patterns of the elliptic and directed flow of  $K^+$  mesons provide independent hints for the existence of a repulsive kaon-nucleon in-medium potential [7,8].

The quantitative study of in-medium effects is complicated by the fact that the  $KN$  potentials depend on the nuclear density, which varies strongly with time during the course of a nucleus-nucleus collision. In order to avoid this complication, one can investigate proton-nucleus collisions where the nuclear density is well defined. Already at saturation density, the in-medium effects are expected to influence strangeness production at beam energies close to the production threshold in  $NN$  collisions (1.58 GeV for  $pp \rightarrow K^+ \Lambda p$  and 2.5 GeV for  $pp \rightarrow K^+ K^- pp$ ). Whereas some data exist on  $K^+$  meson production in proton-nucleus collisions at beam energies between 1.2 and 2.5 GeV pro-

ton kinetic energy [9,10], very little is known about  $K^-$  production in proton-nucleus collisions at threshold beam energies.

So far, only two experiments on antikaon production in proton-nucleus collisions close to threshold energies have been performed. In the experiment in Ref. [11],  $K^-$  mesons were measured at a fixed laboratory angle of  $5.1^\circ$  and at a fixed  $K^-$  momentum of 1.5 GeV/ $c$  using proton kinetic energies of 3.5, 4.0, and 5.0 GeV and light targets (C, Cu), while in the experiment in Ref. [12],  $K^-$  mesons were measured at a fixed laboratory angle of  $10.5^\circ$  and at a fixed  $K^-$  momentum of 1.28 GeV/ $c$  using proton kinetic energies between 2.3 and 2.92 GeV and light targets (Be, Al). In both cases, however, neither the emission angle nor the momentum of the antikaons have been varied, and, accordingly, these data are difficult to interpret.

In order to improve the data situation and to disentangle the above mentioned effects, we performed a systematic investigation of  $K^+$  and  $K^-$  meson production in proton-nucleus collisions. In this Letter, we present results of experiments using proton beams of 1.6, 2.5, and 3.5 GeV kinetic energy impinging on a light and a heavy target. For the first time, the spectral and angular distributions of antikaons have been measured in this energy regime.

The experiments were performed with the Kaon Spectrometer, KaoS, at the heavy-ion synchrotron SIS at Gesellschaft für Schwerionenforschung in Darmstadt [13]. We bombarded C and Au targets (thickness 7 and 2 mm, respectively) with a proton beam having an intensity of up to  $10^{11}$  protons per spill (spill duration  $\sim 10$  s). The emitted charged particles were detected at laboratory angles of

$\theta_{\text{lab}} = 40^\circ, 48^\circ, 56^\circ, \text{ and } 64^\circ$ . By using three settings of the magnetic field, a coverage of laboratory momenta from  $p_{\text{lab}} = 0.3$  to  $1.1$  GeV/ $c$  was obtained.

Figure 1 shows the production cross sections for  $K^+$  and  $K^-$  mesons as a function of their laboratory momentum measured in inclusive proton-carbon (left column) and proton-gold collisions (right column) at 1.6, 2.5, and 3.5 GeV proton kinetic energy (from top to bottom). The laboratory angles are indicated. The error bars represent the statistical uncertainties. An overall systematic error of 15% due to efficiency corrections and beam normalization has to be added.

The lines in Fig. 1 represent a Jüttner-like distribution function

$$E \frac{d\sigma}{d^3p} = \frac{\sigma_{\text{fit}}}{4\pi m_K^2 T K_2(m_K/T)} (p \cdot u) \exp\left(-\frac{p \cdot u}{T}\right), \quad (1)$$

with  $p \cdot u \equiv (E_{\text{lab}} - \beta p_{\text{lab}} \cos\theta_{\text{lab}})/\sqrt{1 - \beta^2}$ , where  $E_{\text{lab}}$  is the  $K^\pm$  energy in the laboratory system and  $\beta$  is the velocity of the kaon emitting source;  $m_K$  denotes the  $K^\pm$  rest mass, and  $K_2$  stands for a modified Bessel function. In a local rest frame ( $\beta = 0$ ), the Jüttner distribution reduces to the known Maxwell-Boltzmann distribution function.

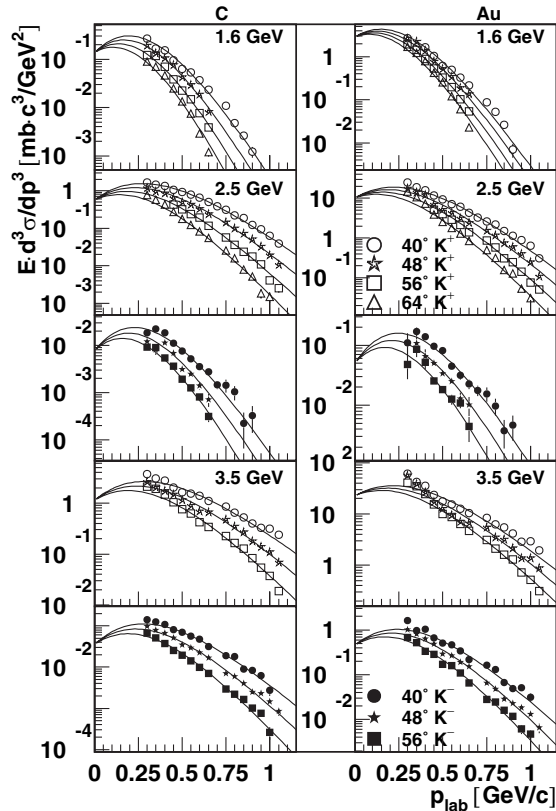


FIG. 1. Invariant production cross sections of  $K^+$  (open symbols) and  $K^-$  mesons (solid symbols) for inclusive proton-carbon (left row) and proton-gold collisions (right row) at 1.6, 2.5, and 3.5 GeV (from top to bottom) as a function of laboratory momentum. The lines correspond to the distribution (1) fitted to the data (see text and Table I).

Expression (1) was fitted simultaneously to the set of differential cross sections measured at different laboratory angles for each system at each energy. In this approach, it is assumed that the particles were emitted isotropically from a source which moves with the velocity  $\beta$  and which has a momentum distribution characterized by a temperature  $T$ . The results of this fitting procedure for the source velocity, the temperature, and the total production cross section  $\sigma_{\text{fit}}$  are listed in Table I. The errors of the fit parameters  $\beta$  and  $T$  are always on the order of 3%–5%. The value of  $\sigma_{\text{fit}}$  is affected by an additional systematic error of 20% due to uncertainties in the relative normalization of the measurements performed at different magnetic field values. This error has to be added to the values of  $\sigma_{\text{fit}}$  given in Table I.

The values of  $\beta$  for proton-nucleus collisions are substantially smaller than the corresponding center-of-mass velocity of the nucleon-nucleon system. This slowing-down of the apparent source velocity may be caused by two effects: (i) The impinging proton collides with a cluster of 2–4 correlated target nucleons, and (ii) the kaons are backscattered at the target nucleus. In both cases, the source velocity  $\beta$  should be larger for proton-carbon than for proton-gold collisions. Indeed, this is observed for  $K^+$  mesons. In the case of  $K^-$  mesons, however, the velocity  $\beta$  is almost independent of the target nucleus mass. This observation indicates that the production process of  $K^-$  mesons is more involved.

The apparent temperature  $T$  is significantly smaller for  $K^-$  mesons than for  $K^+$  for the same collision system. A similar observation was made in nucleus-nucleus collisions at near-threshold beam energies [4]. The interpretation of this effect was related to the delayed emission of  $K^-$  mesons due to strangeness exchange reactions such as  $\pi Y \rightarrow K^- N$ , with  $Y = \Lambda, \Sigma$ .

TABLE I. Beam energy, target,  $K$  meson species, production cross section, source temperature, and source velocity. The values of  $\sigma_{\text{fit}}$ ,  $T$ , and  $\beta$  are obtained by the fitting procedure described in the text. A systematic error of 20% has to be added to the values of  $\sigma_{\text{fit}}$ . The center-of-mass velocity for the nucleon-nucleon system is  $\beta = 0.68, 0.76, \text{ and } 0.81$  for beam energies of 1.6, 2.5, and 3.5 GeV, respectively.

$E_{\text{beam}}$ (GeV)	Target	$K$	$\sigma_{\text{fit}}$ (mb)	$T$ (MeV)	$\beta$
1.6	C	$K^+$	$0.070 \pm 0.006$	45.6	0.48
2.5	C	$K^+$	$0.89 \pm 0.08$	69.9	0.63
3.5	C	$K^+$	$2.04 \pm 0.25$	88.2	0.65
1.6	Au	$K^+$	$0.83 \pm 0.05$	49.0	0.37
2.5	Au	$K^+$	$8.53 \pm 0.95$	73.0	0.53
3.5	Au	$K^+$	$20.74 \pm 1.69$	90.8	0.52
2.5	C	$K^-$	$0.0069 \pm 0.0006$	45.1	0.55
3.5	C	$K^-$	$0.065 \pm 0.007$	65.9	0.64
2.5	Au	$K^-$	$0.059 \pm 0.008$	51.1	0.58
3.5	Au	$K^-$	$0.48 \pm 0.06$	68.1	0.58

In order to visualize the effect of the nuclear medium on strangeness production, we compare our data from proton-nucleus collisions to data measured in proton-proton and nucleus-nucleus collisions. Figure 2 shows the  $K^+$  and  $K^-$  multiplicities  $M_K$  normalized to the number of participating nucleons  $A_{\text{part}}$  as a function of the excess energy. The multiplicity is defined as  $M_K = \sigma_{\text{fit}}/\sigma_R$ , with  $\sigma_R = \pi R^2$  the geometrical reaction cross section. Using  $R = (0.6 + 1.2 \times A^{1/3})$  fm (proton radius 0.6 fm), one obtains  $\sigma_R = 0.35b$  for  $p + C$  and  $\sigma_R = 1.8b$  for  $p + Au$ . The excess energy is defined as the difference between the energy available in a free  $NN$  collision and the  $K^+$  or  $K^-$  production threshold energies in  $NN$  scattering. For  $p + A$  collisions, we define  $A_{\text{part}}$  via the source velocity  $\beta = p_{\text{beam}}/(E_{1\text{beam}} + m_2)$ . Here  $p_{\text{beam}}$  and  $E_{1\text{beam}}$  denote the beam proton momentum and total energy, respectively, and  $m_2$  is the mass of the target nucleons involved in the  $K^\pm$  production. Hence, for  $p + A$  collisions we obtain  $A_{\text{part}} = 1 + m_2/m_N$  with the nucleon mass  $m_N$ . For impact parameter integrated  $A + A$  collisions, the average number of participating nucleons equals  $A/2$ , while for proton-proton collisions we take  $A_{\text{part}} = 2$ .

At beam energies well above threshold, the values of  $M_{K^\pm}/A_{\text{part}}$  from proton-nucleus collisions agree with the ones from proton-proton collisions (represented by the dashed lines). At threshold energies, however, the proton-nucleus data clearly exceed the proton-proton data but undershoot significantly the nucleus-nucleus data. The enhancement of  $M_{K^\pm}/A_{\text{part}}$  when going from  $p + p$ , over  $p + A$ , to  $A + A$  collisions at threshold beam energies is

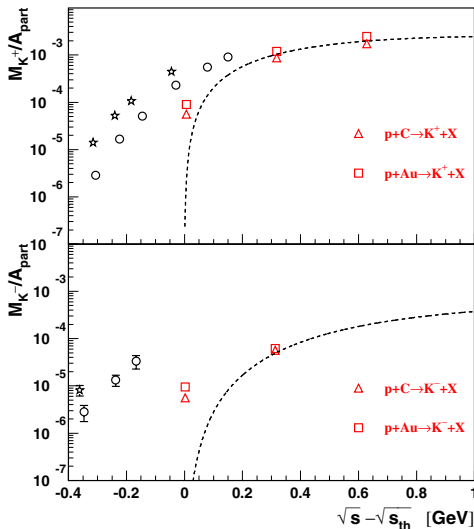


FIG. 2 (color online). Multiplicities of  $K^+$  mesons (upper panel) and  $K^-$  mesons (lower panel) per participating nucleon for proton-carbon (triangles) and proton-gold collisions (squares) as a function of the available energy in the  $NN$  center-of-mass system (i.e., the  $Q$  value). The dashed curves correspond to parametrizations [21] of the measured  $p + p$  data. Data for carbon-carbon (circles) and gold-gold (stars) are taken from Refs. [2,4,22], respectively.

mainly due to Fermi motion, secondary collisions, and increased density. These effects lower the effective thresholds and cause a large difference in  $M_{K^\pm}/A_{\text{part}}$  between  $p + p$  and  $p + A$  but only a moderate difference between  $p + C$  and  $p + Au$ , where the density is comparable. Multiple collisions involving several projectile nucleons can occur only in  $A + A$ . In addition, multiple collisions occur more frequently in  $A + A$  than in  $p + A$  due to the increased density. These effects are nonlinear in  $A_{\text{part}}$  and lead to an enhancement of  $M_{K^\pm}/A_{\text{part}}$  in  $A + A$  collisions with respect to  $p + A$  collisions.

The data presented in Fig. 2 indicate that the enhancement factor between  $p + p$ ,  $p + A$ , and  $A + A$  collisions is significantly larger for  $K^-$  mesons than for  $K^+$  mesons. Such an effect is expected for an increasing contribution of strangeness exchange reactions to  $K^-$  production and for density-dependent in-medium effects.

It is interesting to note that the difference in  $M_{K^-}/A_{\text{part}}$  between  $p + C$  and  $p + Au$  collisions is relatively small, similar to the  $K^+$  mesons. This observation again indicates the important role of strangeness exchange reactions: The yield of  $K^-$  mesons created via strangeness exchange depends only on the abundance of hyperons and not on the numbers of nucleons in the system, as both  $K^-$  production (via  $NY \rightarrow K^- NN$ ) and  $K^-$  absorption (via  $K^- N \rightarrow Y \pi$ ) is proportional to the number of nucleons. Therefore, the target mass dependence of  $K^-$  and  $K^+$  production is very similar.

The interplay of production and absorption of  $K^-$  mesons via strangeness exchange reactions depends on the in-medium properties of the strange particles. For example, a  $K^- N$  potential in the nuclear medium can modify the  $Q$  values for these reactions. In order to study the role of in-medium effects on  $K^-$  production in  $p + A$  collisions more quantitatively, we discuss the ratio

$$R = \left. \frac{d\sigma}{dm_\perp} \right|_{K^-} / \left. \frac{d\sigma}{dm_\perp} \right|_{K^+} \quad (2)$$

of invariant cross sections of inclusive  $K^-$  over  $K^+$  production as a function of the transverse mass in  $p + C$  and  $p + Au$  collisions at an energy of 2.5 GeV (see Fig. 3). The transverse mass  $m_\perp$  is defined as  $\sqrt{p_\perp^2 + m_K^2}$  with  $p_\perp$  the transverse momentum. The data presented in Fig. 3 are integrated over the measured angular range and compared to results of transport model calculations of Boltzmann-Ühling-Uhlenbeck (BUU) type [14]. The BUU calculations take into account the strangeness exchange reactions  $\pi Y \rightarrow K^- N$  and  $NY \rightarrow K^- NN$ . The first channel is dominant in Au + Au collisions. In the C + C system, both channels are about equally important. In proton-nucleus collisions, however, it turns out that the process  $NY \rightarrow K^- NN$  contributes about twice as much to  $K^-$  production as the  $\pi Y \rightarrow K^- N$  reaction. According to the BUU calculations, the strangeness exchange reactions dominate over the direct  $K^-$  production processes, in both nucleus-

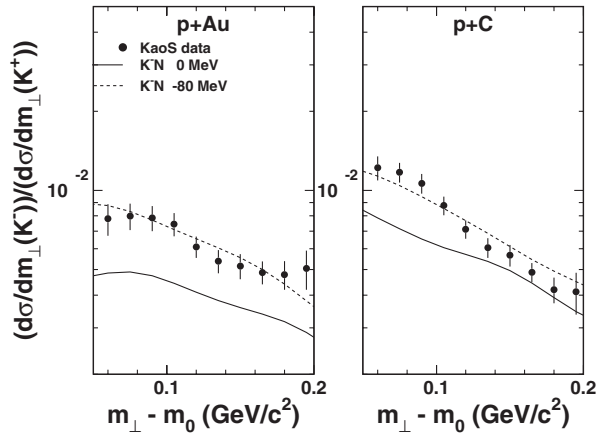


FIG. 3. Ratio of invariant production cross sections of  $K^-$  mesons over  $K^+$  mesons for inclusive proton-gold (left panel) and proton-carbon collisions (right panel) as a function of transverse mass. The data (solid circles) were taken at a beam energy of 2.5 GeV and were integrated over laboratory angles between  $\theta_{\text{lab}} = 36^\circ$  and  $60^\circ$ . The solid and dashed curves depict results of BUU transport model calculations including strangeness exchange as well as a  $K^+N$  potential of +25 MeV. These calculations use  $K^-N$  potentials as indicated.

nucleus and proton-nucleus collisions. For example, in proton-nucleus collisions at 2.5 GeV the contribution of strangeness transfer processes amounts to 50%–60%, and for nucleus-nucleus collisions it is even larger (70%–80%).

In order to discuss density-dependent in-medium potentials, it is important to know at which densities the finally observed  $K^-$  mesons are produced in the various collision systems. For example, for  $p + C$  (Au) collisions at a beam energy of 2.5 GeV, the BUU calculations predict an average density about 0.8 (0.9) times the normal nuclear matter density, whereas for  $C + C$  (Au + Au) collisions the average value is slightly above 1.1 (1.5) times saturation density. The observed  $K^+$  mesons are produced earlier and, hence, at larger average densities: The BUU calculations predict a value of 0.9 (1.0) times normal nuclear matter density for  $p + C$  (Au) collisions, while for  $C + C$  (Au + Au) collisions a value of about 1.4 (2.2) is obtained for the same beam energy.

The data in Fig. 3 (solid dots) are compared to the results of BUU calculations with and without in-medium  $K^-N$  potentials. The theoretical uncertainties in the  $K^+$  production channels—which directly affect the  $K^-$  meson yield via the strangeness exchange reactions—essentially cancel out in the  $K^-/K^+$  ratio. When assuming a  $K^-N$  potential of about  $-80$  MeV (dashed curve in Fig. 3), the calculations agree reasonably well with the  $p + Au$  data and, in average, also for  $p + C$ . The discrepancy between the data and the calculations neglecting  $K^-N$  potentials (solid lines) clearly demonstrates the important role of in-medium effects. Calculations based on momentum dependent potentials as discussed in Ref. [15] yield a similar

agreement with the data for a momentum averaged  $K^-N$  potential of  $-80$  MeV. From the analysis of nucleus-nucleus data, a value of  $-110 \pm 15$  MeV has been obtained for the  $K^-N$  potential at saturation density [5] (see also the compilation in Ref. [16]). A more detailed analysis of our data with respect to in-medium effects calls for an improved theoretical approach, including off-shell effects and in-medium spectral functions [17–20].

In summary, we have presented experimental data on  $K^+$  and  $K^-$  production in  $p + C$  and  $p + Au$  collisions at beam energies close to the production thresholds. This is the first measurement of phase space distributions of anti-kaons in proton induced reactions on nuclei in this energy range. The results presented for  $K^\pm$  production represent an important data set filling the gap between nucleon-nucleon and nucleus-nucleus collisions. The comparison of the data to results of microscopic transport calculations indicate that the in-medium  $K^-N$  potential is on the order of  $-80$  MeV at normal nuclear density.

This work was supported by the German Federal Government (BMBF), by the Polish Committee of Scientific Research (No. 2P3B11515), and by the GSI fund for Universities.

\*Present address: CERN, CH-1211 Geneve 23, Switzerland.

†Present address: Brookhaven National Laboratory, USA.

- [1] R. Barth *et al.*, Phys. Rev. Lett. **78**, 4007 (1997).
- [2] F. Laue *et al.*, Phys. Rev. Lett. **82**, 1640 (1999).
- [3] M. Menzel *et al.*, Phys. Lett. B **495**, 26 (2000).
- [4] A. Förster *et al.*, Phys. Rev. Lett. **91**, 152301 (2003).
- [5] W. Cassing and E. L. Bratkovskaya, Phys. Rep. **308**, 65 (1999).
- [6] G. Q. Li and G. E. Brown, Phys. Rev. C **58**, 1698 (1998).
- [7] Y. Shin *et al.*, Phys. Rev. Lett. **81**, 1576 (1998).
- [8] P. Crochet *et al.*, Phys. Lett. B **486**, 6 (2000).
- [9] M. Debowski *et al.*, Z. Phys. A **356**, 313 (1996).
- [10] V. Koptev *et al.*, Phys. Rev. Lett. **87**, 022301 (2001).
- [11] Y. Sugaya *et al.*, Nucl. Phys. A **634**, 115 (1998).
- [12] Y. Kiselev *et al.*, J. Phys. G **25**, 381 (1999).
- [13] P. Senger *et al.*, Nucl. Instrum. Methods Phys. Res., Sect. A **327**, 393 (1993).
- [14] H. W. Barz and L. Naumann, Phys. Rev. C **68**, 041901 (2003).
- [15] A. Sibirtsev and W. Cassing, Nucl. Phys. A **641**, 476 (1998).
- [16] E. Kolomeitsev *et al.*, J. Phys. G **31**, S741 (2005).
- [17] S. Leupold, Nucl. Phys. A **672**, 475 (2000).
- [18] W. Cassing, L. Tolos, E. L. Bratkovskaya, and A. Ramos, Nucl. Phys. A **727**, 59 (2003).
- [19] L. Tolos, A. Polls, A. Ramos and J. Schaffner-Bielich, Nucl. Phys. A **754**, 356 (2005).
- [20] M. Lutz, Phys. Lett. B **426**, 12 (1998).
- [21] A. Sibirtsev, Phys. Lett. B **359**, 29 (1995); A. Sibirtsev, W. Cassing, and C. M. Ko, Z. Phys. A **358**, 101 (1997).
- [22] C. Sturm *et al.*, Phys. Rev. Lett. **86**, 39 (2001).